https://doi.org/10.5194/amt-2022-94
Preprint. Discussion started: 12 May 2022

Atmospheric Measurement Techniques Discussions

TROPOMI/S5P Total Column Water Vapor Validation against AERONET ground-based measurements

Katerina Garane[1], Ka Lok Chan[2,3], Maria-Elissavet Koukouli[1], Diego Loyola[2], Dimitris Balis[1]

[1]Laboratory of Atmospheric Physics (LAP), Aristotle University of Thessaloniki (AUTH), 54124 Thessaloniki, Greece
[2]Deutsches Zentrum für Luft und Raumfahrt (DLR), Institut für Methodik der Fernerkundung (IMF), 82234 Oberpfaffenhofen, Germany
[3]Rutherford Appleton Laboratory Space (RAL), OX11 0QX Harwell Oxford, United Kingdom

Correspondence to: Katerina Garane (agarane@auth.gr)

Abstract. Water vapor plays a very important role on the greenhouse effect, rendering it an atmospheric constituent that requires continuous and global monitoring by different types of remote sensing instruments. The TROPOMI/S5P Total Column Water Vapor (TCWV) is a new product retrieved from the blue wavelength band (435 –455nm), using an algorithm that was originally developed for the GOME-2/Metop sensors. For the purposes of this work, 2.5 years of continuous satellite observations at high spatial resolution are validated against co-located (in space and in time) precipitable water Level 2.0 (quality-assured) ground-based measurements from the NASA AERONET (AErosol RObotic NETwork). The network uses CIMEL sunphotometers located at approximately 1300 stations globally to monitor precipitable water among other products. The two datasets, satellite and ground-based, were co-located and the percentage differences of the comparisons were calculated and statistically analyzed. The correlation coefficient of the two products is found to be 0.9 and the mean bias of the relative percentage differences is of the order of only -3 % for the mid-latitudes and the tropics (±60°). The effect of various influence quantities, such as air mass factor, solar zenith angle, clouds and albedo are also presented and discussed. It was found that the cloud properties affect the validation results, leading the TCWV to a dry bias of -19 % for low cloudiness (CTP > 800hPa). The cloud albedo introduces a wet bias of 10 % when the cloud albedo is below 0.3 and a dry bias up to -20 % when the clouds are more reflective. Overall, the TROPOMI/S5P TCWV product, on a global scale and for moderate albedo and cloudiness, agrees well at -4.0 ± 4.3 % with the ground-truth.

1 Introduction

The greenhouse effect, i.e., the infrared radiation energy trapped within the earth-atmosphere system by atmospheric gases and clouds, is found to be highly dependent on the amount of water vapor in the atmosphere (Raval et al., 1989). Water vapor is a natural greenhouse gas that originates from the evaporation of the earth's water and absorbs the heat radiated by the earth. Its presence in the atmosphere follows a cycle that consists of cloud formation via condensation, transportation and return to the earth's surface by precipitation, as rain or snow. It has a major positive feedback, ranging from 1.1 $Wm^{-2}K^{-1}$ to 2.4 $Wm^{-2}K^{-1}$, with a mean value of 1.7 $Wm^{-2}K^{-1}$, hence its effect on global warming can be double the CO_2 contribution

https://doi.org/10.5194/amt-2022-94
Preprint. Discussion started: 12 May 2022


Atmospheric Measurement Techniques Discussions

(Colman, 2003). The way that water vapor affects the climate's energy balance is very nicely described by Inamdar and Ramanathan (1998): following the warming of the earth's surface and the troposphere by the increasing levels of CO_2 and other greenhouse gases, the water vapor content of the atmosphere also increases and further contributes to the greenhouse effect, therefore to the atmosphere's warming. Therefore, water vapor strongly determines the atmosphere's response to surface warming. Nevertheless, under certain circumstances it is conceivable that negative feedback could result from the increase of the water vapor content in the atmosphere, hence the increase in cloudiness, that could lead to the cooling of the atmosphere. It is evident that the net effect that water vapor changes can have on the climate is not clear yet.

Additionally, water vapor as a chemical compound has another very crucial role in the atmosphere since it is the origin of the tropospheric hydroxyl radical, which is a significant oxidant in the troposphere, and affects the ozone depletion in the stratosphere over high latitude areas (Dlugokencky et al., 2016).

Being such an important key-factor for the greenhouse effect evolution and the projection of future climate changes, water vapor is an atmospheric constituent that requires continuous and global monitoring by different types of remote sensing instruments and in individual spectral bands, such as microwave, short wave infrared and visible bands.

The TROPOMI/S5P Total Column Water Vapor (TCWV) is a new global product retrieved from the blue wavelength band (435 –455nm). The retrieval algorithm was further developed by the German Aerospace Center (DLR) within the framework of the European Space Agency's (ESA's) Sentinel 5 Precursor Product Algorithm Laboratory (S5P-PAL), using as a basis the algorithm that was originally developed for the GOME-2 (Global Ozone Monitoring Experiment-2) sensors TCWV products. The GOME-2 algorithm (Chan et al., 2020) was adjusted in terms of spectral analysis, air mass factor calculations and new surface albedo retrieval approach (Chan et al., 2022).

Schneider et al. (2020) introduced the retrieval of a clear sky TCWV product retrieved from a different TROPOMI/S5P wavelength band, namely from its short-wave infrared (2305-2385 nm) observations. The product retrieval was further developed by Schneider et al. (2022) to also cover cloudy scenes and was validated against co-located ground-based Fourier transform infrared (FTIR) observations by the Total Carbon Column Observing Network (TCCON). The validation results showed that for mid-latitude stations under clear sky conditions the satellite product has a 1.8 % bias with respect to TCCON, which becomes 8.8 % for cloudy scenes.

The objective of this work is to validate the TROPOMI/S5P TCWV product retrieved from the blue band. For our validation purposes, the co-located precipitable water Level 2.0 (cloud screened, quality-assured and calibrated) ground-based measurements from the NASA AERONET (https://aeronet.gsfc.nasa.gov/, AErosol RObotic NETwork; Giles et al., 2019), were used. The network uses CIMEL spectral Sun photometers, which are automatic, solar powered and self-calibrating instruments that robotically scan the sun and the sky and measure atmospheric aerosol optical properties and precipitable water (Holben et al., 1998). The AERONET database provides precipitable water observations at approximately 1300 stations globally.

In Sect. 2, the characteristics of the available satellite and ground-based data used in this work are given. Sect. 3 describes the co-location methodology as well as the ground-based dataset quality control protocols. Sect. 4 presents the global

https://doi.org/10.5194/amt-2022-94
Preprint. Discussion started: 12 May 2022


Atmospheric Measurement Techniques Discussions

validation results of TROPOMI/S5P TCWV and a discussion about the dependence of the satellite product on various influence quantities. Finally, a summary and the conclusions are given in Sect. 5.

2 Data sources

2.1 TROPOMI/S5P total column water vapor

The TROPOspheric Monitoring Instrument (TROPOMI, http://www.tropomi.eu/) on board the Copernicus Sentinel-5 Precursor (S5P) was launched in November 2017, monitoring the earth's atmosphere using four spectrometers with spectral bands in the ultraviolet (UV), the visible (UVIS), the near-infrared (NIR) and the shortwave infrared (SWIR) wavelengths (Veefkind et al., 2012). The observations are performed in a sun-synchronous low-earth orbit with a local equatorial crossing time of 13:30 LT and daily global coverage with 14 orbits per day. Its spatial resolution was 3.5 km (across-track) by 7.0 km (along track) up to 6th August 2019, when it was modified to 3.5 km (across-track) by 5.5 km (along track). Its swath width is 2600 km, consisting of 450 ground pixels across-track which provides daily global coverage. The TROPOMI instrument and its pre-launch calibration techniques are thoroughly described by Kleipool et al. (2018), while the in-flight calibration is analyzed in Ludewig et al. (2020).

The TROPOMI/S5P Total Column Water Vapor (TCWV) is a new product retrieved from the sensor's observations in the visible blue band (435 –455nm). The retrieval algorithm, thoroughly described in Chan et al. (2022), is based on the GOME-2 TCWV algorithm (Chan et al., 2020), which is utilizing the Differential Optical Absorption Spectroscopy (DOAS) technique. In short, the two steps approach is followed: first retrieving slant columns through the spectral analysis of the TROPOMI measurements in the blue band, and then converting the slant columns to vertical columns using an iterative air mass factor (AMF) calculation. Compared to the GOME-2 algorithm, some improvements were applied concerning the spectral retrieval, the air mass factors calculations and the surface albedo input parameter, for which the GE_LER (Geometry-dependent effective Lambertian equivalent reflectivity) that is produced by TROPOMI (Loyola et al., 2020), is used. Finally, the cloud information (e.g., cloud fraction, cloud top pressure and cloud albedo) are taken from the TROPOMI operational cloud product (Loyola et al., 2018). According to Chan et al. (2022), TROPOMI/S5P reports lower TCWV values by 1.24 kg/m^2 over land compared to ERA5 TCWV reanalysis data, and by 1.74 kg/m^2 with respect to GOME-2 observations. Additionally, they report that the uncertainty of TCWV observations over the tropics is 10-19 % under clear skies (effective cloud fraction < 0.5).

For this work, 2.5 years (May 2018 to December 2020) of continuous TCWV satellite observations were made available. The data were provided in NetCDF format, each file containing one orbit (14 files/orbits per day) and they were filtered according to Chan et al. (2022) following the filtering criteria: (a) solar zenith angle <85°, (b) effective cloud fraction <0.5, (c) Root Mean Square fit residual <0.002 and (d) Air Mass Factor >0.1.

Figure 1 shows four seasonal global maps of the TROPOMI/S5P TCWV: panel (a) depicts the winter months December to February; panel (b) the spring months March to May; panel (c) the summer months June to August and panel (c) the autumn

https://doi.org/10.5194/amt-2022-94
Preprint. Discussion started: 12 May 2022

Atmospheric Measurement Techniques Discussions

months September to November. Throughout the year, the tropics hold the higher TCWV content, up to 80 kg/m^2 occurring mainly during summer and autumn. Over land in the Northern Hemisphere, where most of the ground-based stations are located, the TCWV is below 50 kg/m^2, decreasing closer to the poles below 5-10 kg/m^2.

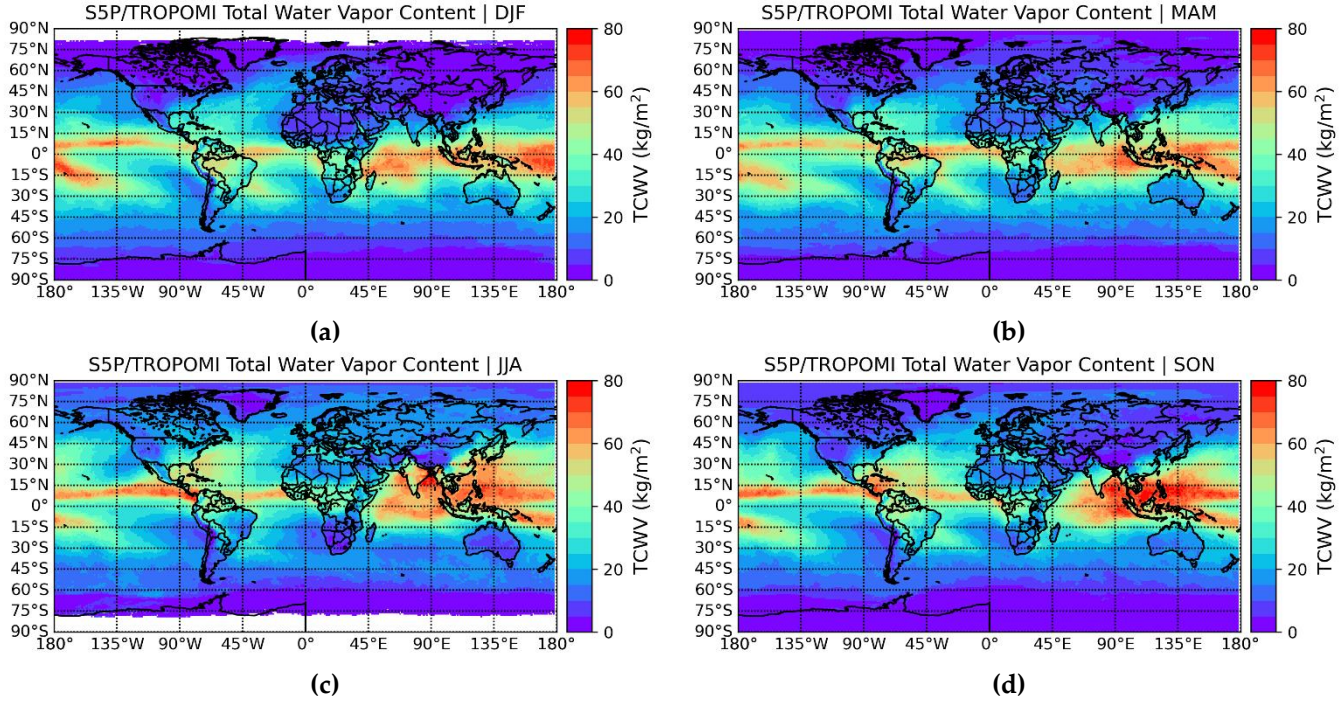

Figure 1: Seasonal global maps of the TROPOMI/S5P TCWV product (in kg/m2). Panel (a): December – February; panel (b): March – May; panel (c): June – August and panel (d): September – November

2.2 Ground-based observations

The database used as ground-truth for the S5P TCWV validation consists of archived Cimel precipitable water observations that were downloaded from the AERONET website (https://aeronet.gsfc.nasa.gov/). The network uses Cimel Sun photometers located at about 1300 stations globally to monitor precipitable water, among other products, every 15 minutes. The Cimel instruments perform direct sun measurements when the optical path between the instrument and the sun is cloud-free. The AERONET processing algorithm Version 3 (Giles et al., 2019) was used for the retrieval and it is stated within the archived data files that "the data are automatically cloud cleared and quality assured with pre-field and post-field calibration applied". AERONET data are provided in three quality levels, namely 1.0, 1.5 and 2.0 (https://aeronet.gsfc.nasa.gov/new_web/aot_levels_versions.html):

- Level 1.0 data use the pre-field deployment sun calibration.
- Level 1.5 data use Level 1.0 data and apply a cloud-screening and automatic quality control procedures.
- Data are raised to Level 2.0 after applying the final post-field deployment sun calibration to Level 1.5 data.

Here, Level 2 precipitable water observations were utilized to achieve the best possible quality for the ground-truth.

https://doi.org/10.5194/amt-2022-94
Preprint. Discussion started: 12 May 2022

Atmospheric Measurement Techniques Discussions

The AERONET dataset covers about 25-30 years of measurements, depending on the station, and it was extensively used for the MODIS water vapor products validation (Bennouna et al., 2013; Diedrich et al., 2015; Bright et al., 2018; Shi et al., 2018; Martins et al., 2019). Schneider et al. (2010) found that Cimel instruments have a clear sky dry bias, which is larger in winter (25.5 %), decreasing during spring (11.5 %), and becomes a minor wet bias (-2 %) in the summer months. The seasonality in the dry bias of the Cimel observations is caused by their restriction to clear-sky measurements. The AERONET precipitable water vapor product was evaluated by Pérez-Ramírez et al. (2014), where it was compared to water vapor retrievals from radiosonde observations and other ground-based retrieval techniques, such as microwave radiometry (MWR) and GPS for a few sites. It was found that the AERONET precipitable water has a dry bias of approximately 5–6 % in the retrievals and a total estimated uncertainty of 12–15 %. Weaver et al. (2017) also intercompared water vapor measurements performed by different types of instruments, namely radiosondes, sunphotometers, FTIR spectrometers and a microwave radiometer, at the Eureka, Nunavut, site. They showed that the sunphotometers operated at two nearby sites report lower water vapor observations compared to co-located FTIR or Atmospheric Emitted Radiance Interferometer (AERI) instruments, by 15 % or 3.3 %, respectively. According to Martins et al. (2019), the total uncertainty of sun photometer retrievals was estimated to be less than 10 % (Smirnov et al., 2004; Alexandrov et al., 2009), which was expected to be improved with the implementation of the version 3 of the retrieval algorithm (Giles et al., 2019). The extended network of automatic and quality-controlled observations, providing very dense (spatially and temporally) coverage of all continents, in addition to the homogeneity of the retrieval algorithms, are very strong advantages in favor of the AERONET use for this validation work.

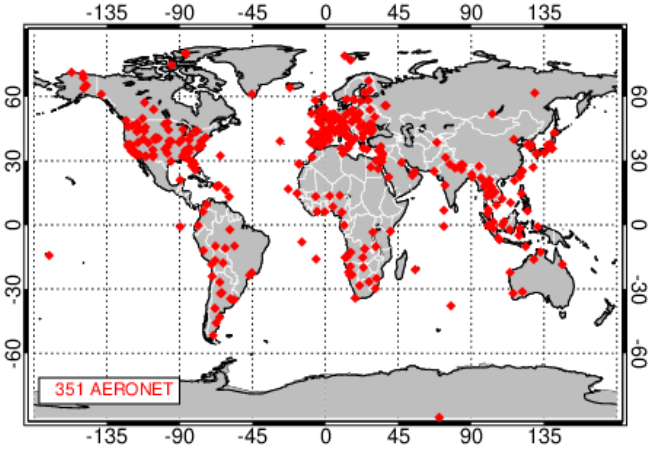

Figure 2: Spatial distribution of the 351 AERONET ground-based stations used for the comparisons to TROPOMI/S5P TCWV product.

https://doi.org/10.5194/amt-2022-94
Preprint. Discussion started: 12 May 2022

Atmospheric Measurement Techniques Discussions

The data files retrieved from AERONET are available in ASCII format in daily, monthly or instantaneous temporal analysis. Here, the instantaneous precipitable water observations were used, for the time period May 2018 to December 2020, depending on the availability of data for each individual station. Out of the 1304 stations, only 596 reported Level 2 precipitable water measurements after 2017. An in-house quality control resulted to the reduction of the number of stations to be used for the validation of TROPOMI/S5P TCWV down to 351. Nevertheless, the final number of stations is still enough to cover all continents, as it can be seen in Figure 2.

3. Co-location methodology and AERONET stations quality control

Following the generation of the satellite overpass files for each station that include all relevant parameters for each TCWV measurement, a co-location methodology was applied using the AERONET ground-based measurements as a basis for the comparisons. Specifically, pairs of co-located satellite and instantaneous ground-based measurements were formed, and their percentage difference was calculated. The co-location criteria applied to minimize the noise of the comparisons were:

- the maximum search radius between the ground-based station and the center co-ordinates of the satellite pixel was set to 10 km, and
- the satellite and ground-based instantaneous TCWV absolute difference in measurement time had to be up to 30'.

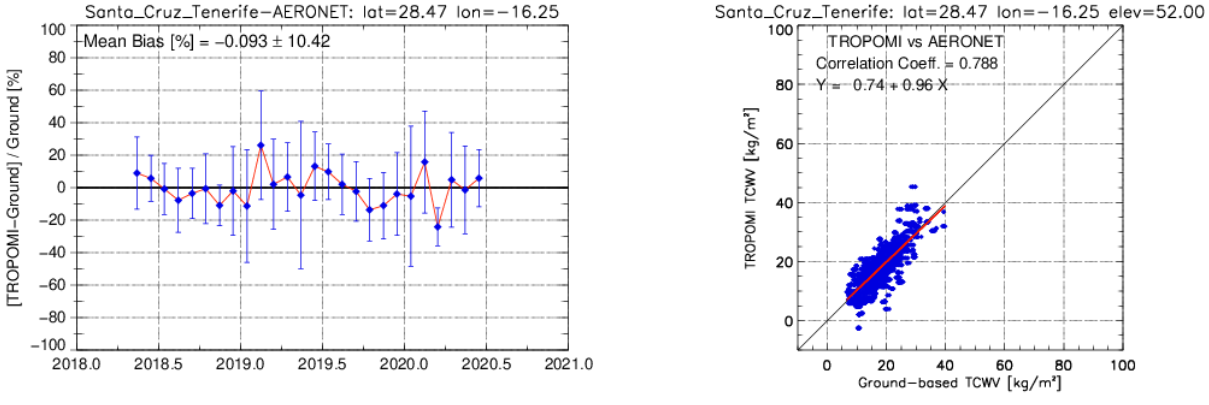

(**a**) (**b**)

Figure 3: The monthly mean percentage differences between satellite and ground-based observations (panel a) and the respective scatter plot (panel b) for an indicative Northern Hemisphere station, Santa Cruz, Tenerife.

https://doi.org/10.5194/amt-2022-94
Preprint. Discussion started: 12 May 2022

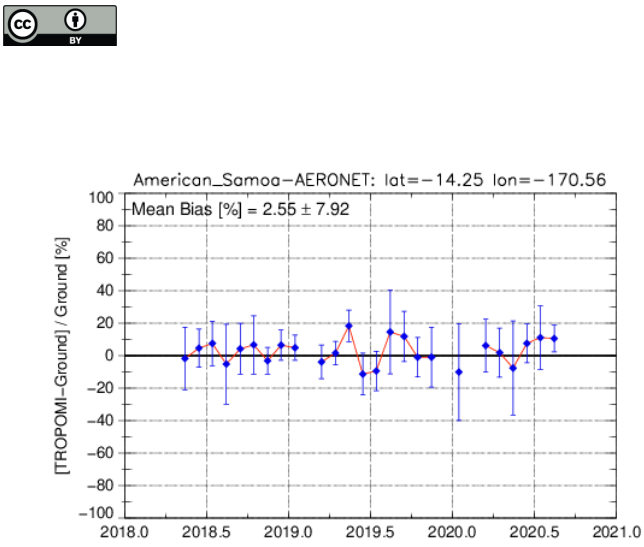

(a)

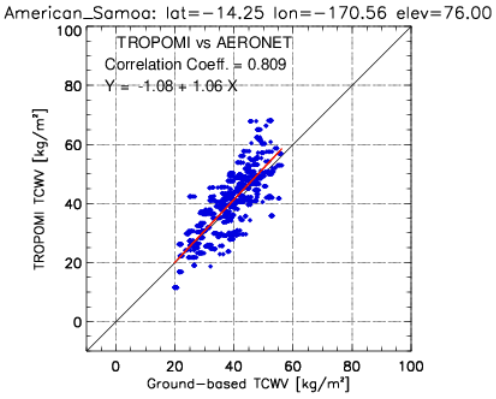

(b)

Figure 4: The same as Figure 3, for the Southern Hemisphere station American Samoa, located at the South Pacific Ocean.

After co-locating the two datasets, a per-station analysis was performed for all ground-based stations with available co-locations to decide on the number of stations to be used for this work, depending on the station's data quality and quantity. As an example, the validation results for two individual stations located at different latitudes are shown in Figure 3 and Figure 4. Panels (a) show the monthly mean percentage differences between satellite and ground-based observations for the two indicative stations from the Northern (Figure 3) and the Southern Hemisphere (Figure 4), namely Santa Cruz, Tenerife and American Samoa, South Pacific Ocean. The error bars represent the 1σ standard deviation of the means. Panels (b) show the respective scatter plots per station. These two stations are very nice examples of good quality and continuous ground-based measurements. It can be seen from these figures already that the correlation between ground-based and satellite TCWV observations is very good, above 0.79. The slope of the linear fits is 0.96 and 1.06 respectively, while the offset is 0.74 (Figure 3) and -1.08 kg/m^2 (Figure 4). The mean relative bias per station (panels a) depends strongly on the ground-based instrument's calibration, but for the examples shown here they are within ±2.6 %, showing a very good agreement between satellite and ground-based observations and a good temporal stability of both sources of measurement.

https://doi.org/10.5194/amt-2022-94
Preprint. Discussion started: 12 May 2022

Atmospheric Measurement Techniques Discussions

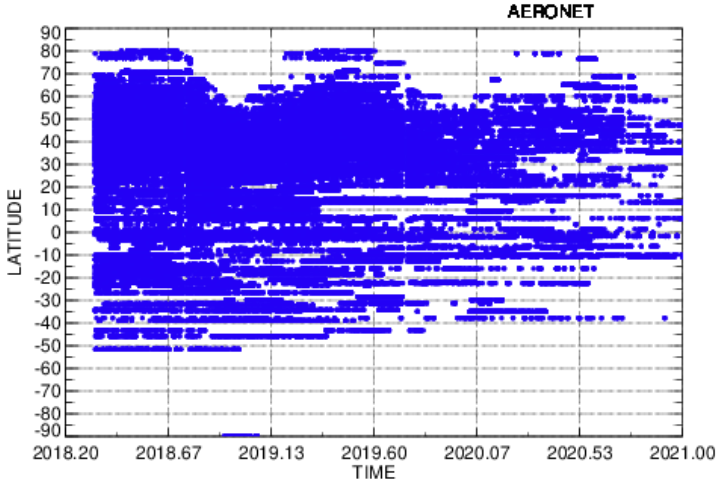

Figure 5: Spatial and temporal representation of the co-location data used for the validation with ground-based measurements for the time period of the TROPOMI/S5P TCWV data availability (May 2018 to December 2020).

In Figure 5, the distribution of the about 633.000 co-locations in space and in time, is shown. Most stations upload their Level 2 data to the AERONET with some delay after observation, which is the reason for the limited number of available co-locations for the most recent months of the validation period. This is even more pronounced in the Southern Hemisphere, where the number of available stations is smaller, and they extend down to 55° S. There is only one station below that latitude, namely the South Pole Observatory (latitude 90° S), with available measurements that cover a very short time period of two months during 2018. Therefore, concerning the Southern Hemisphere we can only draw conclusions for the latitude belt from the equator down to 60° S. The Northern high latitude co-locations (above 75° N) are available for the summer months of 2018 and 2019 and there are only a few observations for the summer months of 2020.

The monthly means that are shown in the respective time series plots in this work, are calculated by averaging the total number of available instantaneous co-locations per month. The same stands for every averaging quantity plotted here: the mean values are always computed by averaging all individual co-locations that fall within the bin in question. Henceforward, the error bars in the plots (where they are shown) stand for the standard error of the mean with a confidence interval (CI) of 99.7% for each mean value. As it is expected, since there is a plethora of co-locations, the standard error frequently results to an extremely small value, showing the very good accuracy of the averaging.

https://doi.org/10.5194/amt-2022-94
Preprint. Discussion started: 12 May 2022

Atmospheric Measurement Techniques Discussions

4. Discussion on the validation analysis

4.1. Global comparisons between TROPOMI/S5P TCWV and AERONET ground-based observations

In this section, the archived and quality-controlled AERONET water vapor observations, for the period May 2018 – December 2020, are used for the validation of TROPOMI/S5P TCWV in a global scale. Figure 6 shows the global statistics of the about 633.000 co-located data. The histogram to the left (panel a), shows that the overall mean relative percentage difference between satellite and ground-based measurements is only -4.0 %, the 1σ standard deviation is 43.6 % and the standard error is 0.2 %. The distribution of the percentage differences around the mean value is a normal Gaussian. The scatter plot to the right (panel b), which has a correlation coefficient of 0.91, shows the very good overall agreement between the two datasets. The slope of the linear fit is 0.89 and the overall offset between satellite and ground-based observations is 0.9 kg/m^2.

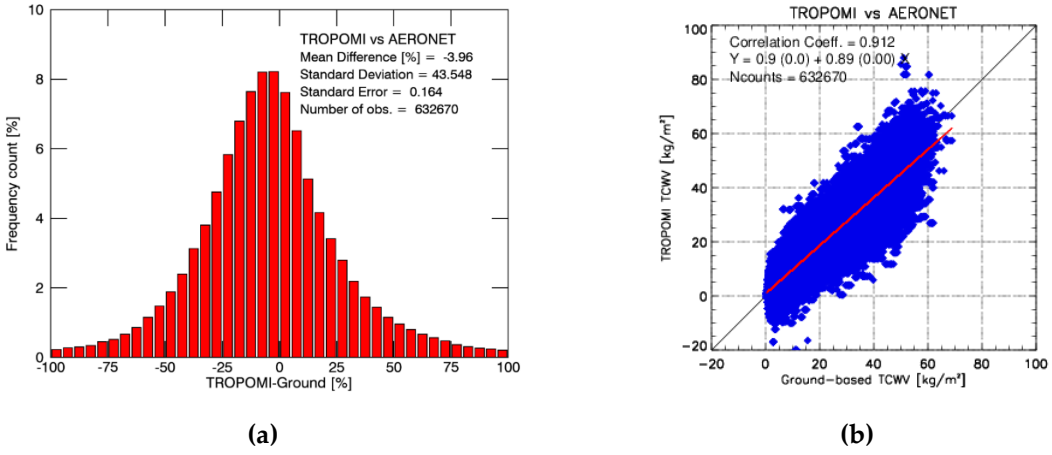

(a) **(b)**

Figure 6: (a) The distribution of the satellite and ground-based co-location percentage differences. (b) The scatter plot showing the correlation between TROPOMI/S5P TCWV and the AERONET observations.

To study the temporal evolution of the comparisons, the co-located data are divided into two time-series, depending on the station's latitude. Figure 7 shows the time series of the monthly mean percentage differences between satellite and instantaneous co-located (in space and in time) ground-based measurements: in the left panel (a) the Northern Hemisphere (NH) time series is shown, while in the right panel (b) the respective comparisons for the Southern Hemisphere (SH) are depicted, with their standard errors shown as error bars at the 99.7% CI. The NH curve is continuous with no abrupt changes, showing the temporal stability of both sources of measurement, satellite and ground-based. The same applies to the SH until 2020, when the number of available AERONET data for this part of the earth is reduced, causing the increase of the variability and the standard error of the means seen since June 2020. The mean relative bias of the percentage differences for the NH, where the stations density is very high, was found to be -4.7 ± 2.2 % and the respective mean standard error of the

https://doi.org/10.5194/amt-2022-94
Preprint. Discussion started: 12 May 2022

Atmospheric Measurement Techniques Discussions

available monthly means is 1.0 %. In the SH, the mean bias is smaller but more variable, +0.5 ± 5.8 %, mainly representing the latitude belt 0° to 60° S. The reduced number of co-locations after June 2020, results in a higher overall mean standard error of 2.6 %. Table 1 summarizes the global and hemispheric statistics of the monthly mean analysis.

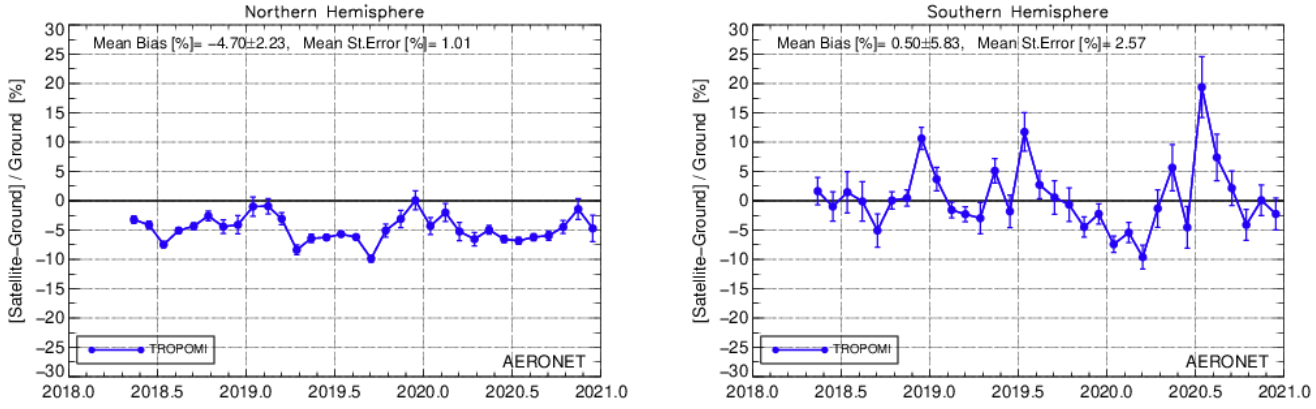

(a) **(b)**

Figure 7: The time series of the monthly mean percentage differences between TROPOMI/S5P TCWV and ground-based AERONET measurements, shown for the Northern (panel a) and the Southern Hemisphere (panel b).

Table 1: The monthly mean global and hemispheric statistics of the co-located satellite and ground-based observations.

	NH	SH	Globally
Mean Bias	-4.7 ± 2.3 %	+0.5 ± 5.8 %	-4.0 ± 4.3 %
Standard Error (99.7 % CI)	1.0 %	2.6 %	0.2 %
Co-locations	531 000	102 000	633 000

https://doi.org/10.5194/amt-2022-94
Preprint. Discussion started: 12 May 2022

Atmospheric Measurement Techniques Discussions

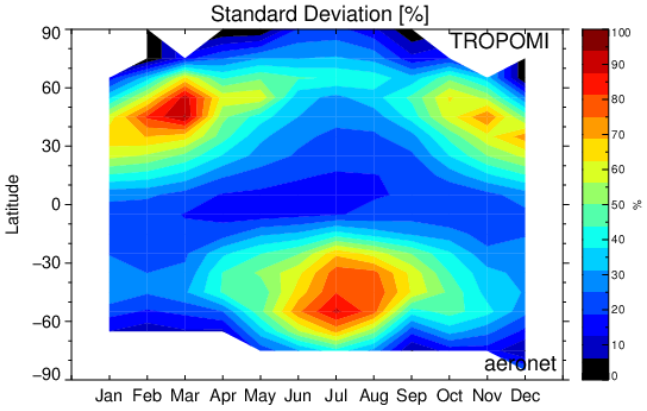

Figure 8: The seasonal and latitudinal variability of the standard deviations (in %) of the mean percentage differences between satellite and ground-based TCWV observations.

Table 2: The zonal statistics of the co-located satellite and ground-based observations

Hemisphere	Latitude belt	Mean Diff.[1] (kg/m^2)	Mean Rel. Bias (%)	Mean St. Dev. (%)	Mean St. Err.[2] (%)
NH	90°-60°	-0.4	1.2 ± 31.5	61.3	12.6
	60°-30°	-0.8	-4.0 ± 2.9	44.0	1.3
	30°-15°	-2.2	-5.9 ± 3.4	23.6	1.6
	15°-0°	-3.7	-9.6 ± 3.0	18.5	2.0
SH	0°-15°	-2.5	-5.9 ± 5.5	32.2	3.3
	15°-30°	-0.7	2.4 ± 8.3	52.3	3.6
	30°-60°	+0.5	5.8 ± 12.3	46.1	8.9
	60°-90°	+0.3	42.2 ± 4.9	84.8	16.5

[1] Satellite-Ground

[2] 99.7% CI

The contour plot in Figure 8 shows the standard deviation of the percentage differences between satellite and ground-based co-locations with respect to latitude and season. The plot depicts the strong seasonality of the comparisons' standard deviations, i.e. of their variability, which is high during the winter months of each hemisphere (up to 100 %), and low (10-30 %) during summer, when the number of ground-based AERONET measurements (i.e. the number of co-locations) and their accuracy is much higher (Fragkos et al., 2019). The seasonal dependency of the standard deviation originates mostly from the latitude belts 15°-70° of both hemispheres, which are the most station-populated. Additionally, as shown in Figure 1, for

https://doi.org/10.5194/amt-2022-94
Preprint. Discussion started: 12 May 2022


Atmospheric Measurement Techniques Discussions

latitudes higher than the tropics of both hemispheres the water vapor content is lower and has a stronger temporal variability, explaining the higher standard deviations of the percentage differences. It is also very interesting to see that the variability of the comparisons for the tropics (Fig. 8, 15° N-15° S) is much smaller compared to the other latitude belts, showing the very good and temporally invariable agreement between the two sources of information in this part of the globe. The statistics per latitude belt in terms of mean difference (satellite – ground) in kg/m^2, relative bias, mean standard deviation and mean standard error of the comparisons (in %), are shown in Table 2.

In Figure 9, panel (a), the mean percentage differences per station with available ground-based data are averaged in 10° latitude belts and are shown versus latitude. The same is shown in panel (b), but the averaged quantity per latitude bin is the difference between satellite and ground-based observations in kg/m^2. The overall mean relative percentage bias for the latitudinal dependency is 0.6 ± 13.6 % and has a mean standard error of 3.1 %. When only the co-locations northwards 50° S are considered, the statistics for the mean bias become -1.4 ± 7.4 % and the mean standard error is reduced to 2.6 %. The agreement between satellite and ground-based observations is very good, remaining within ± 10% for individual belts of the NH and the belt above 50° of the SH. The latitude bins -30° S to 30° N form a slight U-shaped curve, showing that the satellite instrument reports lower TCWV up to ~10 % with respect to ground-based observations for the stations close to the equator. This result, which corresponds to a difference between satellite and ground-based observations up to -4 kg/m^2 (panel b), is in agreement with Chan et al. (2022), where the dry bias is attributed to albedo effects in the visible band over vegetation and to the presence of aerosol and/or clouds in the measurement field. For the NH high latitude stations, above 70° N, the discrepancy becomes positive up to 14 % (panel a). In terms of difference (panel b), this percentage accounts for a very small overestimation of ~1 kg/m^2 by TROPOMI/S5P, since the amount of water vapor close to the poles is less than 20 kg/m^2 (see Figure 1). Likewise, for the latitude bin 80° S-90° S, where only the South Pole station is contributing with observations, the mean bias is very high, 42 %, but the respective difference of the measurements is only 0.3 kg/m^2.

It is worth noting that the mean relative bias of each latitude bin and the respective mean standard deviation, thus the variability (not shown in Figure 9), should not be attributed to the satellite product only, since it is well known that some ground-based stations may overestimate or underestimate TCWV systematically, mainly due to their calibration. Most of the spurious ground-based observations were filtered out of the ground-truth database used in this validation work. Nevertheless, for some latitude bins, like 50° S-60° S and below 80° S (including only the South Pole Observatory station), where the station density or the temporal coverage is very low, the respective stations were considered with the remark that their co-locations statistics should be interpreted with caution. Nevertheless, as shown above, there is no clear pattern in the dependency of the percentage differences on latitude, even though there is an indication of an underestimation close to the equator that turns into a minor overestimation close to the poles. Considering that the uncertainties of both types of measurement is ~10%, the comparison of the satellite and ground-based observations is regarded very good. Howbeit, the performance of the TROPOMI/S5P TCWV retrieval algorithm, mainly on the aspect of the surface albedo parameter credibility appears to be sound.

https://doi.org/10.5194/amt-2022-94
Preprint. Discussion started: 12 May 2022

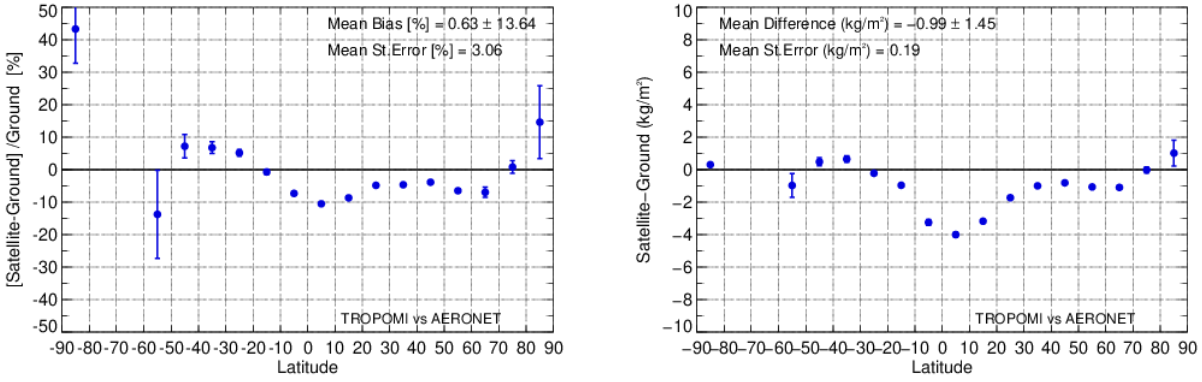

(a) **(b)**

Figure 9: Panel (a): The percentage differences between co-located TROPOMI/S5P TCWV measurements and ground-based observations from AERONET instruments plotted versus latitude. Panel (b): As in panel (a) but for the differences between satellite and ground-based observations in kg/m².

4.2 Discussion on the dependence of TROPOMI/S5P TCWV on various geophysical influence quantities

In this section, the dependence of the validation results on various influence quantities is investigated. These quantities can be parameters that are used as inputs for the TCWV retrieval algorithm, such as cloud and surface information, or detailed results like air mass factor. To inspect any possible dependences, all available co-locations are averaged in bins regarding the quantity in question. Note that the numbers at the top of each figure show the number of co-locations that are averaged for each bin, and they appear only for those bins for which the number of co-locations is less than 3% of the total. This is a way to distinguish the data points in terms of relative importance.

4.2.1. Viewing geometry

Figure 10 shows the dependency of the percentage differences on solar zenith angle (SZA – panel a) and viewing zenith angle (VZA – panel b).

Regarding the dependency on SZA (panel a), TROPOMI/S5P reports lower TCWV than the AERONET observations by ~-5.5 % for SZAs below 45°, where almost half of the co-locations are included. Their difference is eliminated for SZAs 45°-80° and slightly increases with SZA, reaching +8 % above 80°. Overall, the dependence of the percentage differences on SZA is ~13%. As expected, the standard error of the means increases for higher SZAs because of the increase in the uncertainty of the measurements, the lower number of co-locations and of course due to the strong effect of the winter mid-latitude co-locations. On the contrary, no systematic dependence of the comparisons on VZA (panel b) is seen.

https://doi.org/10.5194/amt-2022-94
Preprint. Discussion started: 12 May 2022

Atmospheric Measurement Techniques Discussions

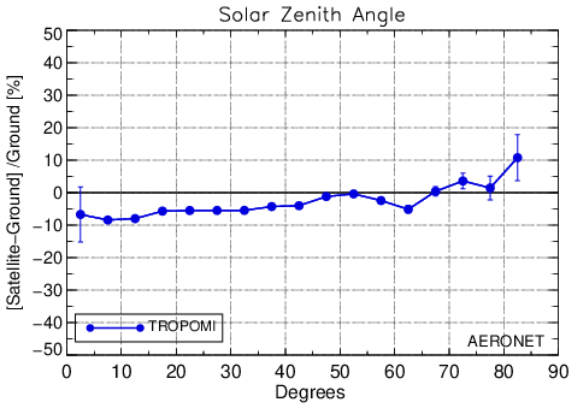

(a)

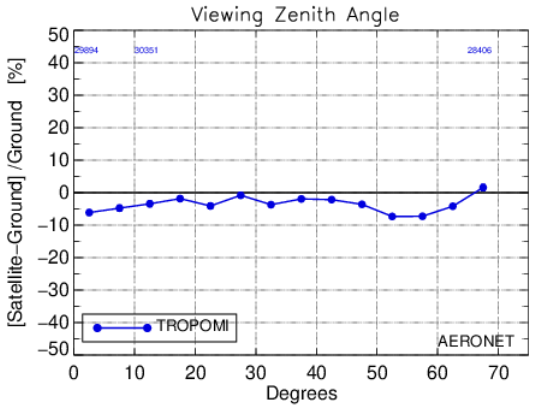

(b)

Figure 10: The dependence of the percentage differences on solar zenith angle (a) and viewing zenith angle (b).

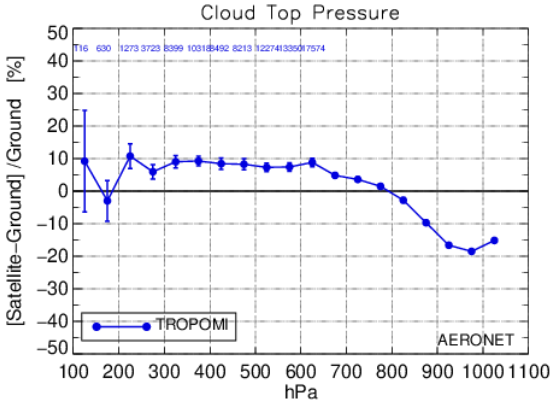

(a)

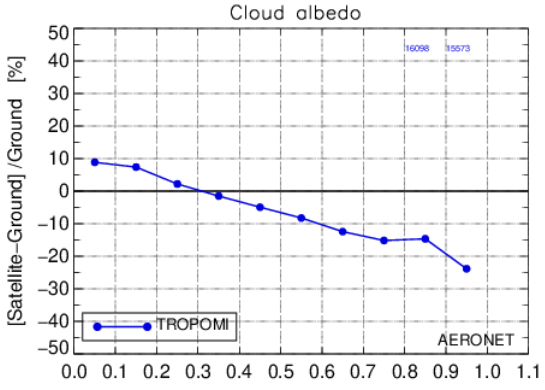

(b)

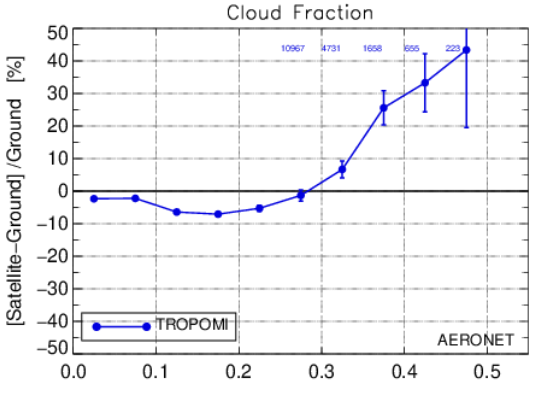

(c)

Figure 11: The dependency of the comparisons of satellite to ground-based TCWV measurements on three different cloud parameters, namely: (a) cloud top pressure; (b) cloud albedo and (c) cloud fraction.

https://doi.org/10.5194/amt-2022-94
Preprint. Discussion started: 12 May 2022


Atmospheric Measurement Techniques Discussions

4.2.2. Input data

The TCWV retrieval algorithm requires two categories of input data that are simultaneously retrieved from TROPOMI/S5P measurements: the cloud properties and the surface properties.

Concerning the cloud properties retrieved with the OCRA/ROCINN algorithms (Loyola et al., 2018), Figure 11 shows the dependence of the comparisons on cloud top pressure (panel a), cloud albedo (panel b) and cloud fraction (panel c). As is indicated from the figures, the satellite TCWV has a noticeable dependence on cloud pressure and cloud albedo:

- For cloud pressures up to 800 hPa, the comparisons have an almost stable positive bias of ~ +6 %, which decreases to -18 % when the pressure increases to ~1000 hPa, hence for lower clouds which may also affect the ground-based measurements.
- Panel b shows that the comparisons have a strong overall dependence of 30 % on cloud albedo. The bias of the comparisons is positive, +10 % maximum, for cloud albedo values below 0.3 and becomes negative, up to -20 %, for increasing cloud albedo, thus for brighter clouds.
- The cloud fraction figure (panel c) shows that the vast majority of the co-locations have cloud fraction values below 0.3, which is expected since both satellite and ground-based observations are filtered for cloudiness. Within the cloud fraction range of 0 to 0.3, no particular dependence is seen. The filtering of the co-location dataset for cloud fraction less than 0.3 was also investigated, resulting to no major differences in the validation results.

Overall, the dependence of the percentage differences on cloud fraction and cloud albedo could also be an issue of the ghost total column, i.e., the water vapor that may be present beneath the clouds but not properly measured by the satellite instrument, when even a part of the sky is cloudy. The fact that the ground-based measurements are screened for cloudiness and the satellite observations are allowed to have a part of the measurement field covered with clouds, can be another cause for the small differences seen between them.

The dependence of the comparisons on surface properties retrieved with the GE_LER algorithm (Loyola et al., 2020), namely surface pressure and surface albedo, is shown in Figure 12.

- Surface pressure (panel a): for the typical range of surface pressures i.e., 900 – 1050 hPa, no dependence is seen in the comparisons. As expected, the bins with pressures less than 900 hPa have a very limited number of co-locations and the curve represents mostly noise data.
- Surface albedo (panel b): As the density of ground-based stations is much higher at the mid-latitudes of both hemispheres, very few co-locations have surface albedo above 0.2. Above this value, the comparisons have no apparent systematic dependence on surface albedo, showing mainly increased noise. The surface albedo range 0.9-1.0 has a few co-locations coming from the South Pole Observatory, which explains the high discrepancy between satellite and ground-based observations.

https://doi.org/10.5194/amt-2022-94
Preprint. Discussion started: 12 May 2022

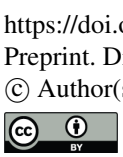

Atmospheric Measurement Techniques Discussions

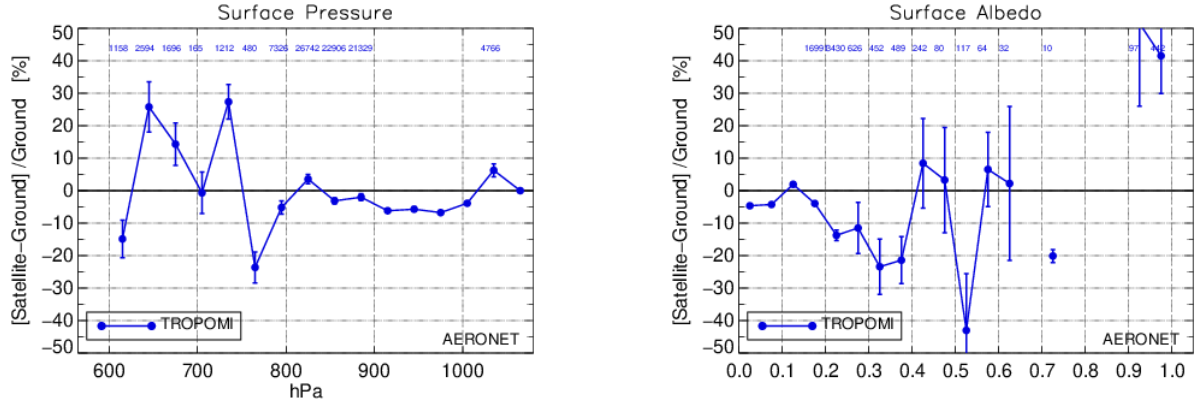

(**a**) (**b**)

Figure 12: The dependence of the comparisons of satellite to ground-based TCWV measurements on two surface parameters, namely: (a) surface pressure and (b) surface albedo.

4.2.3. Detailed results

The parameters given as detailed results of the retrieval algorithm in the satellite data files are the following:

- Air Mass Factor (AMF). The dependence of the percentage differences of co-located data on AMF is shown in Figure 13, panel a. For the well-populated bins with AMF ranging between 0.8 and 2 the bias is negligible, which is expected since the measurements acquired under low SZAs have also a bias of 0 to -5.5 % (Figure 10, panel a). For AMF values between 2 and 4 the bias becomes negative, up to -18 %, probably affected by the cloudiness, while for AMF greater than 4 the number of co-locations per averaged bin is very low and their variability is not considered statistically important.
- Root Mean Square error of fit (RMS). Figure 13, panel b, shows no systematic dependence on RMS, even for the bins with low number of co-locations.
- Water Vapor Slant Column Density (SCD). Figure 13, panel c, shows the dependence on the Water Vapor SCD result. No dependence of the comparisons on the specific parameter is seen when the algorithm retrieves values above 10 kg/m^2. The limited number of co-locations with positive SCD values below 10 kg/m^2 have a percentage difference of -30 %. Negative SCDs are mainly due to measurement noise. By analyzing the spectral fit residual, the random uncertainty of SCD retrieval is typically <1kg/m^2. Although this error is small, it could cause a significant impact over area with low atmospheric water vapor content and result in negative values. In addition, this effect can be further amplified when the AMF is small (below 1). Even though they are very few in population, should be treated with caution since they have extremely high percentage differences with respect to ground-based measurements, approximately -100 %.

https://doi.org/10.5194/amt-2022-94
Preprint. Discussion started: 12 May 2022

Atmospheric Measurement Techniques Discussions

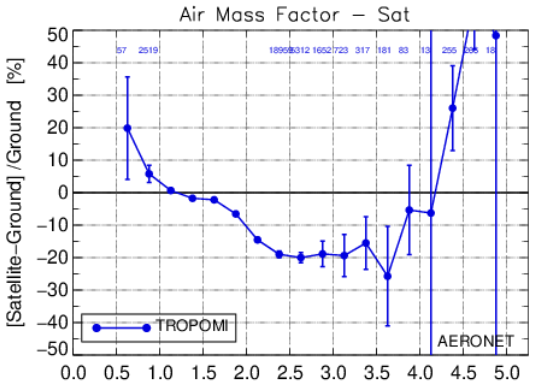

(a)

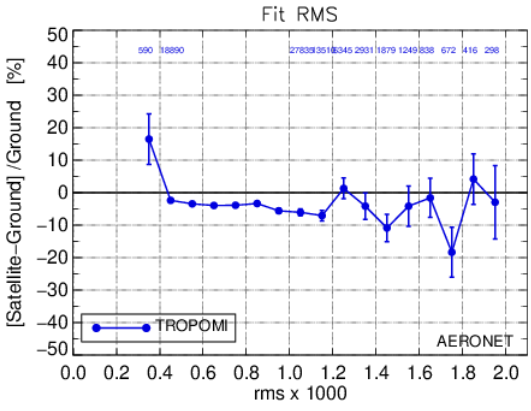

(b)

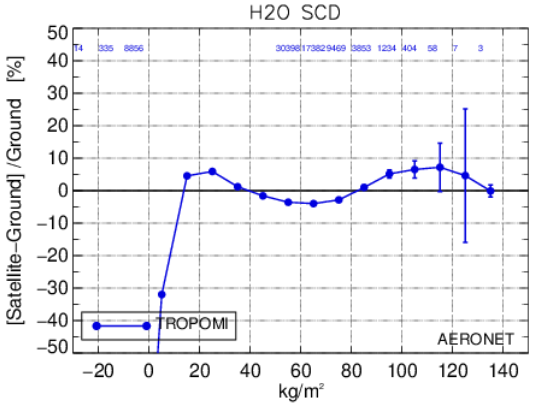

(c)

Figure 13: The dependence of the comparisons of satellite to ground-based TCWV measurements on three parameters, namely: (a) air mass factor; (b) RMS and (c) water vapor slant column density.

5. Summary statistics and conclusions

The main purpose of this work is to examine the performance of the new TCWV product retrieved from the blue band of the TROPOMI/S5P observations and their consistency to AERONET ground-based measurements. About 630.000 instantaneous co-located data were available during the time period May 2018 to December 2020, coming from 351 ground-based stations and the respective satellite overpasses. The percentage differences that were calculated from the co-located pairs of data with temporal difference up to 30' and maximum search radius up to 10 km, correspond to clear-skies observations (cloud fraction <0.5) and were statistically analyzed in terms of temporal and latitudinal dependences. Furthermore, their dependence on various influence quantities was investigated. The validation results can be summarized to the following:

https://doi.org/10.5194/amt-2022-94
Preprint. Discussion started: 12 May 2022


Atmospheric Measurement Techniques Discussions

- The overall mean percentage difference between TROPOMI/S5P and AERONET TCWV observations is only -4.0 %, while their correlation coefficient is excellent, 0.91. When the two hemispheres are studied separately, their mean bias results to -4.7 % for the NH and +0.5 % for the SH. Considering that the uncertainty of the satellite TCWV product is ~ 10-19 %, and the ground-based measurements' uncertainty is reported to be ~10 %, the agreement between the two datasets is deemed very satisfactory. The mean standard error of the comparisons, at a 99.7% CI, is 0.2 %, showing the very good accuracy of the results. Additionally, considering the dry bias of the AERONET observations that was discussed in Sect. 2.2 and which is about -5 to -10 % (depending on the study and its reference) and varies with season and latitude, it can be concluded that the satellite TCWV observations have a dry bias with respect to the "absolute" truth of about -9 to -13 %, respectively.
- A seasonal pattern was found for the standard deviation of the mid-latitude monthly mean percentage differences, being rather limited (~10-30%) during summer when the number of available ground-based measurements is higher and their uncertainty lower. The standard deviation is increased (up to 70 – 100 %) during the winter months of each hemisphere. A zonal analysis of the monthly mean percentage differences and their standard deviations showed that this effect comes mainly from the most station-populated latitude belts, i.e. 15°-60° of both hemispheres. The respective standard deviations for the tropics (15° N-15° S), where the bulk of the water vapor is concentrated, is much lower and temporally stable, about ± 20 %, showing a reduced variability of the comparisons between satellite observations and ground-truth.
- The pole-to-pole analysis of the co-locations showed that there is a negative mean bias seen for the tropics, up to -10 % or -4 kg/m^2 close to the equator, which is an indication of TCWV dry bias induced by the satellite with respect to the ground-truth. The opposite results when assessing the high latitude co-locations (above 70°), where the mean bias is 14 % for the Northern Hemisphere and 42 % for the Southern Hemisphere. Nevertheless, these high percentages result from very small differences (~0.3-1 kg/m^2) occurring at high latitudes where the amounts of water vapor are significantly lower.
- Finally, many quantities influencing the satellite retrievals were studied, and no particular dependences were found, except for a dependency on cloud top pressure (CTP) and cloud albedo. Specifically, it resulted that for low cloudiness (CTP > 800 hPa) the satellite reports lower TCWV by up to -19 % compared to the ground-based measurements. The dependency on cloud albedo is strong, about 30 %, showing a wet bias of 10 % when the cloud albedo is below 0.3 and a dry bias up to -20 % when the clouds are more reflective (albedo > 0.3).

To conclude, as shown from the ground-based validation of 2.5 years of available satellite observations, the TROPOMI/S5P TCWV product retrieved from the blue spectral range, is a product of high quality and precision, temporally stable and not affected by any other parameters, except from clouds when and if some cloudiness at lower atmospheric layers is present in the measurement field. This product is expected to substantially contribute to a very long time series of total column water vapor climate data record achieved by utilizing other blue band satellites along with TROPOMI/S5P.

https://doi.org/10.5194/amt-2022-94
Preprint. Discussion started: 12 May 2022


Atmospheric Measurement Techniques Discussions

Data availability: The TROPOMI/S5P TCWV data were retrieved using the algorithm described in Chan et al. (2022). The dataset is foreseen to be available through the ESA Sentinel 5 Precursor Product Algorithm Laboratory (S5P-PAL) framework. The AERONET ground-based Level 2.0 precipitable water measurements were downloaded from https://aeronet.gsfc.nasa.gov/.

Author contribution: Conceptualization by KG and DB. The validation methodology was defined by KG and MEK. The scripts used for the analysis were written by KG and MEK. The data analysis and validation was performed by KG, MEK and DB. KLC and DL provided the satellite data. KG wrote the manuscript. MEK, DB, DL and KLC reviewed and edited the manuscript. Project administration by DL. Funding acquisition by DL and DB. All authors have read and agreed to the published version of the manuscript.

Competing interests: The authors declare that they have no conflict of interest.

Acknowledgements: We thank the AERONET PI(s) and Co-I(s) and their staff for establishing and maintaining the 351 sites used in this investigation. We thank the European Space Agency (ESA) for supporting the TROPOMI/S5P TCWV optimization within the framework of Sentinel 5 Precursor Product Algorithm Laboratory (S5P-PAL) project.

Financial Support: This research was funded by the German Aerospace Center (DLR) in coordination with the DLR Innovative Products for Analyses of Atmospheric Composition (INPULS) project.

References

Alexandrov, M. D., Schmid, B., Turner, D. D., Cairns, B., Oinas, V., Lacis, A. A., Gutman, S. I., Westwater, E. R., Smirnov, A. and Eilers, J.: Columnar water vapor retrievals from multifilter rotating shadowband radiometer data, J. Geophys. Res., 114, D02306, https://doi.org/10.1029/2008JD010543, 2009.

Bennouna, Y. S., Torres, B., Cachorro, V. E., Ortiz de Galisteo, J. P. and Toledano, C.: The evaluation of the integrated water vapour annual cycle over the Iberian Peninsula from EOS-MODIS against different ground-based techniques, Q. J. R. Meteorol. Soc., 139 (676), 1935–1956, https://doi.org/10.1002/qj.2080, 2013.

Bright, J. M., Gueymard, C. A., Killinger, S., Lingfors, D., Sun, X., Wang, P. and Engerer, N. A.: Climatic and global validation of daily MODIS precipitable water data at AERONET sites for clear-sky irradiance modelling, In Proceedings of the EuroSun 2018 Conference on Solar Energy and Buildings, Rapperswil, Switzerland, 10 - 13 September 2018.

Chan, K. L., Valks, P., Slijkhuis, S., Köhler, C. and Loyola, D.: Total column water vapor retrieval for Global Ozone Monitoring Experience-2 (GOME-2) visible blue observations, Atmos. Meas. Tech., 13, 4169–4193, https://doi.org/10.5194/amt-13-4169-2020, 2020.

Chan, K. L., Xu, J., Slijkhuis, S., Valks, P. and Loyola, D.: TROPOspheric Monitoring Instrument observations of total column water vapour: Algorithm and validation, Science of The Total Environment, Volume 821, 153232, ISSN 0048-9697, https://doi.org/10.1016/j.scitotenv.2022.153232, 2022.

Colman, R.: A comparison of climate feedbacks in general circulation models, Climate Dynamics, 20, 865–873, https://doi.org/10.1007/s00382-003-0310-z, 2003.

Diedrich, H., Preusker, R., Lindstrot, R. and Fischer, J.: Retrieval of daytime total columnar water vapour from MODIS measurements over land surfaces, Atmos. Meas. Tech., 8, 823–836, https://doi.org/10.5194/amt-8-823-2015, 2015.

Dlugokencky, E., Houweling, S., Dirksen, R., Schröder, M., Hurst, D., Forster, P., and WMO Secretariat: Observing Water Vapour, World Meteorological Organization (WMO), Bulletin nº: Vol 65 (2)-2016, available online at https://public.wmo.int/en/resources/bulletin/observing-water-vapour (accessed on 23 February 2022), 2016.

Fragkos, K., Antonescu, B., Giles, D. M., Ene, D., Boldeanu, M., Efstathiou, G. A., Belegante, L. and Nicolae, D.: Assessment of the total precipitable water from a sun photometer, microwave radiometer and radiosondes at a continental site in southeastern Europe, Atmos. Meas. Tech., 12, 1979–1997, https://doi.org/10.5194/amt-12-1979-2019, 2019.

Giles, D. M., Sinyuk, A., Sorokin, M. G., Schafer, J. S., Smirnov, A., Slutsker, I., Eck, T. F., Holben, B. N., Lewis, J. R., Campbell, J. R., Welton, E. J., Korkin, S. V. and Lyapustin, A.I.: Advancements in the Aerosol Robotic Network (AERONET) Version 3 database – automated near-real-time quality control algorithm with improved cloud screening for Sun photometer aerosol optical depth (AOD) measurements, Atmos. Meas. Tech., 12, 169-209, https://doi.org/10.5194/amt-12-169-2019, 2019.

Holben, B. N., Eck, T. F., Slutsker, I., Tanré, D., Buis, J. P., Setzer, A., Vermote, E., Reagan, J. A., Kaufman, Y. J., Nakajima, T., Lavenu, F., Jankowiak, I. and Smirnov, A., AERONET—A Federated Instrument Network and Data Archive for Aerosol Characterization, Remote Sensing of Environment, 66, Issue 1, 1-16, ISSN 0034-4257, https://doi.org/10.1016/S0034-4257(98)00031-5, 1998.

Inamdar, A.K. and Ramanathan, V.: Tropical and global scale interactions among water vapor, atmospheric greenhouse effect, and surface temperature, J. Geophys. Res., 103(D24), 32177– 32194. https://doi.org/10.1029/1998JD900007, 1998.

Kleipool, Q., Ludewig, A., Babi´c, L., Bartstra, R., Braak, R., Dierssen, W., Dewitte, P.-J., Kenter, P., Landzaat, R., Leloux, J., Loots, E., Meijering, P., van der Plas, E., Rozemeijer, N., Schepers, D., Schiavini, D., Smeets, J., Vacanti, G., Vonk, F., Köehler, P., Frankenberg, C., Magney, T.S., Guanter, L., Joiner, J. and Landgraf, J.: Global retrievals of solar-induced chlorophyll fluorescence with TROPOMI: First results and intersensory comparison to OCO-2, Geophys. Res. Lett., 45, 10456–10463, https://doi.org/10.1029/2018GL079031, 2018.

Loyola, D. G., Gimeno García, S., Lutz, R., Argyrouli, A., Romahn, F., Spurr, R. J. D., Pedergnana, M., Doicu, A., Molina García, V. and Schüssler, O.: The operational cloud retrieval algorithms from TROPOMI on board Sentinel-5 Precursor, Atmos. Meas. Tech., 11, 409–427, https://doi.org/10.5194/amt-11-409-2018, 2018.

Loyola, D. G., Xu, J., Heue, K.-P. and Zimmer, W.: Applying FP_ILM to the retrieval of geometry-dependent effective Lambertian equivalent reflectivity (GE_LER) daily maps from UVN satellite measurements, Atmos. Meas. Tech., 13, 985–999, https://doi.org/10.5194/amt-13-985-2020, 2020.

Ludewig, A., Kleipool, Q., Bartstra, R., Landzaat, R., Leloux, J., Loots, E., Meijering, P., van der Plas E., Rozemeijer, N., Vonk, F. and Veefkind, P.: In-flight calibration results of the TROPOMI payload on board the Sentinel-5 Precursor satellite, Atmos. Meas. Tech., 13, 3561–3580, https://doi.org/10.5194/amt-13-3561-2020, 2020

Martins, V.S., Lyapustin, A., Wang, Y., Giles, D. M., Smirnov, A., Slutsker, I. and Korkin, S.: Global validation of columnar water vapor derived from EOS MODIS-MAIAC algorithm against the ground-based AERONET observations, Atmospheric Research, Volume 225, Pages 181-192, ISSN 0169-8095, https://doi.org/10.1016/j.atmosres.2019.04.005, 2019.

Pérez-Ramírez, D., Whiteman, D. N., Smirnov, A., Lyamani, H., Holben, B.N., Pinker, R., Andrade, M. and Alados-Arboledas, L.: Evaluation of AERONET precipitable water vapor versus microwave radiometry, GPS, and radiosondes at ARM sites, J. Geophys. Res. Atmos., 119, 9596–9613, https://doi.org/10.1002/2014JD021730, 2014.

Raval, A. and Ramanathan, V.: Observational determination of the greenhouse effect, Nature, 342, 758–761, https://doi.org/10.1038/342758a0, 1989.

Schneider, M., Romero, P. M., Hase, F., Blumenstock, T., Cuevas, E. and Ramos, R.: Continuous quality assessment of atmospheric water vapour measurement techniques: FTIR, Cimel, MFRSR, GPS, and Vaisala RS92, Atmos. Meas. Tech., 3, 323–338, https://doi.org/10.5194/amt-3-323-2010, 2010.

Schneider, A., Borsdorff, T., aan de Brugh, J., Aemisegger, F., Feist, D. G., Kivi, R., Hase, F., Schneider, M., and Landgraf, J.: First data set of H2O/HDO columns from the Tropospheric Monitoring Instrument (TROPOMI), Atmos. Meas. Tech., 13, 85–100, https://doi.org/10.5194/amt-13-85-2020, 2020.

Schneider, A., Borsdorff, T., aan de Brugh, J., Lorente, A., Aemisegger, F., Noone, D., Henze, D., Kivi, R., and Landgraf, J.: Retrieving H2O/HDO columns over cloudy and clear-sky scenes from the Tropospheric Monitoring Instrument (TROPOMI), Atmos. Meas. Tech., 15, 2251–2275, https://doi.org/10.5194/amt-15-2251-2022, 2022.

Shi, F., Xin, J., Yang, L., Cong, Z., Liu, R., Ma, Y., Wang, Y., Lu, X. and Zhao, L.: The first validation of the precipitable water vapor of multisensor satellites over the typical regions in China, Remote Sens. Environ., 206, 107–122, https://doi.org/10.1016/j.rse.2017.12.022, 2018.

Smirnov, A., Holben, B. N., Lyapustin, A., Slutsker, I. and Eck., T. F.: AERONET Processing Algorithms Refinement, AERONET Workshop, El Arenosillo, Spain, 10-14 May 2004

Veefkind, J. P., Aben, I., McMullan, K., Förster, H., de Vries, J., Otter, G., Claas, J., Eskes, H. J., de Haan, J. F., Kleipool, Q., van Weele, M., Hasekamp, O., Hoogeveen, R., Landgraf, J., Snel, R., Tol, P., Ingmann, P., Voors, R., Kruizinga, B., Vink, R., Visser, H. and Levelt, P.F.: TROPOMI on the ESA Sentinel-5 Precursor: A GMES mission for global observations

https://doi.org/10.5194/amt-2022-94
Preprint. Discussion started: 12 May 2022


Atmospheric Measurement Techniques Discussions

of the atmospheric composition for climate, air quality and ozone layer applications, Remote Sens. Environ., 120, 70–83, https://doi.org/10.1016/j.rse.2011.09.027, 2012.

Weaver, D., Strong, K., Schneider, M., Rowe, P. M., Sioris, C., Walker, K. A., Mariani, Z., Uttal, T., McElroy, C. T., Vömel, H., Spassiani, A., and Drummond, J. R.: Intercomparison of atmospheric water vapour measurements at a Canadian High Arctic site, Atmos. Meas. Tech., 10, 2851–2880, https://doi.org/10.5194/amt-10-2851-2017, 2017